12-1998

Measurement of triple gauge WWγ couplings at LEP2 using photonic events

R. BARATE

Manoj THULASIDAS

Singapore Management University, manojt@smu.edu.sg

EUROPEAN LABORATORY FOR PARTICLES PHYSICS (CERN)

CERN-EP/98-178
16 November 1998

Measurement of triple gauge WWγ couplings at LEP2 using photonic events.

The ALEPH Collaboration *)

Abstract

A study of events with photons and missing energy has been performed with the data sample obtained with the ALEPH detector at centre-of-mass energies from 161 to 184 GeV, corresponding to a total integrated luminosity of about 80 pb^{-1}. The measured distributions are in agreement with Standard Model predictions, leading to constraints on WWγ gauge coupling parameters $\Delta\kappa_\gamma$ and λ_γ. The results from the fit to the cross sections and to the energy and angular distributions of the photons are:

$$\begin{aligned} \Delta\kappa_\gamma &= 0.05^{+1.15}_{-1.10}(\mathrm{stat}) \pm 0.25(\mathrm{syst}) \\ \lambda_\gamma &= -0.05^{+1.55}_{-1.45}(\mathrm{stat}) \pm 0.30(\mathrm{syst}). \end{aligned}$$

(Submitted to Physics Letters B)

*) See next pages for the list of authors

The ALEPH Collaboration

R. Barate, D. Buskulic, D. Decamp, P. Ghez, C. Goy, S. Jezequel, J.-P. Lees, A. Lucotte, F. Martin, E. Merle, M.-N. Minard, J.-Y. Nief, P. Perrodo, B. Pietrzyk

Laboratoire de Physique des Particules (LAPP), IN^{2}P^3-CNRS, F-74019 Annecy-le-Vieux Cedex, France

R. Alemany, M.P. Casado, M. Chmeissani, J.M. Crespo, M. Delfino, E. Fernandez, M. Fernandez-Bosman, Ll. Garrido,[15] E. Graugès, A. Juste, M. Martinez, G. Merino, R. Miquel, Ll.M. Mir, P. Morawitz, A. Pacheco, I.C. Park, A. Pascual, I. Riu, F. Sanchez

Institut de Física d'Altes Energies, Universitat Autònoma de Barcelona, 08193 Bellaterra (Barcelona), E-Spain[7]

A. Colaleo, D. Creanza, M. de Palma, G. Gelao, G. Iaselli, G. Maggi, M. Maggi, S. Nuzzo, A. Ranieri, G. Raso, F. Ruggieri, G. Selvaggi, L. Silvestris, P. Tempesta, A. Tricomi,[3] G. Zito

Dipartimento di Fisica, INFN Sezione di Bari, I-70126 Bari, Italy

X. Huang, J. Lin, Q. Ouyang, T. Wang, Y. Xie, R. Xu, S. Xue, J. Zhang, L. Zhang, W. Zhao

Institute of High-Energy Physics, Academia Sinica, Beijing, The People's Republic of China[8]

D. Abbaneo, U. Becker,[22] G. Boix,[2] M. Cattaneo, F. Cerutti, V. Ciulli, G. Dissertori, H. Drevermann, R.W. Forty, M. Frank, F. Gianotti, A.W. Halley, J.B. Hansen, J. Harvey, P. Janot, B. Jost, I. Lehraus, O. Leroy, C. Loomis, P. Maley, P. Mato, A. Minten, L. Moneta,[20] A. Moutoussi, N. Qi, F. Ranjard, L. Rolandi, D. Rousseau, D. Schlatter, M. Schmitt,[1] O. Schneider, W. Tejessy, F. Teubert, I.R. Tomalin, E. Tournefier, M. Vreeswijk, H. Wachsmuth

European Laboratory for Particle Physics (CERN), CH-1211 Geneva 23, Switzerland

Z. Ajaltouni, F. Badaud G. Chazelle, O. Deschamps, S. Dessagne, A. Falvard, C. Ferdi, P. Gay, C. Guicheney, P. Henrard, J. Jousset, B. Michel, S. Monteil, J-C. Montret, D. Pallin, P. Perret, F. Podlyski

Laboratoire de Physique Corpusculaire, Université Blaise Pascal, IN^{2}P^3-CNRS, Clermont-Ferrand, F-63177 Aubière, France

J.D. Hansen, J.R. Hansen, P.H. Hansen, B.S. Nilsson, B. Rensch, A. Wäänänen

Niels Bohr Institute, 2100 Copenhagen, DK-Denmark[9]

G. Daskalakis, A. Kyriakis, C. Markou, E. Simopoulou, A. Vayaki

Nuclear Research Center Demokritos (NRCD), GR-15310 Attiki, Greece

A. Blondel, J.-C. Brient, F. Machefert, A. Rougé, M. Rumpf, R. Tanaka, A. Valassi,[6] H. Videau

Laboratoire de Physique Nucléaire et des Hautes Energies, Ecole Polytechnique, IN^{2}P^3-CNRS, F-91128 Palaiseau Cedex, France

E. Focardi, G. Parrini, K. Zachariadou

Dipartimento di Fisica, Università di Firenze, INFN Sezione di Firenze, I-50125 Firenze, Italy

R. Cavanaugh, M. Corden, C. Georgiopoulos, T. Huehn, D.E. Jaffe

Supercomputer Computations Research Institute, Florida State University, Tallahassee, FL 32306-4052, USA [13,14]

A. Antonelli, G. Bencivenni, G. Bologna,[4] F. Bossi, P. Campana, G. Capon, V. Chiarella, P. Laurelli, G. Mannocchi,[5] F. Murtas, G.P. Murtas, L. Passalacqua, M. Pepe-Altarelli[12]

Laboratori Nazionali dell'INFN (LNF-INFN), I-00044 Frascati, Italy

M. Chalmers, L. Curtis, J.G. Lynch, P. Negus, V. O'Shea, B. Raeven, C. Raine, D. Smith, P. Teixeira-Dias, A.S. Thompson, E. Thomson, J.J. Ward

Department of Physics and Astronomy, University of Glasgow, Glasgow G12 8QQ,United Kingdom[10]

O. Buchmüller, S. Dhamotharan, C. Geweniger, P. Hanke, G. Hansper, V. Hepp, E.E. Kluge, A. Putzer, J. Sommer, K. Tittel, S. Werner,[22] M. Wunsch

Institut für Hochenergiephysik, Universität Heidelberg, D-69120 Heidelberg, Germany[16]

R. Beuselinck, D.M. Binnie, W. Cameron, P.J. Dornan,[12] M. Girone, S. Goodsir, N. Marinelli, E.B. Martin, J. Nash, J.K. Sedgbeer, P. Spagnolo, M.D. Williams

Department of Physics, Imperial College, London SW7 2BZ, United Kingdom[10]

V.M. Ghete, P. Girtler, E. Kneringer, D. Kuhn, G. Rudolph

Institut für Experimentalphysik, Universität Innsbruck, A-6020 Innsbruck, Austria[18]

A.P. Betteridge, C.K. Bowdery, P.G. Buck, P. Colrain, G. Crawford, G. Ellis, A.J. Finch, F. Foster, G. Hughes, R.W.L. Jones, A.N. Robertson, M.I. Williams

Department of Physics, University of Lancaster, Lancaster LA1 4YB, United Kingdom[10]

P. van Gemmeren, I. Giehl, C. Hoffmann, K. Jakobs, K. Kleinknecht, M. Kröcker, H.-A. Nürnberger, G. Quast, B. Renk, E. Rohne, H.-G. Sander, S. Schmeling, C. Zeitnitz, T. Ziegler

Institut für Physik, Universität Mainz, D-55099 Mainz, Germany[16]

J.J. Aubert, C. Benchouk, A. Bonissent, J. Carr,[12] P. Coyle, A. Ealet, D. Fouchez, F. Motsch, P. Payre, M. Talby, M. Thulasidas, A. Tilquin

Centre de Physique des Particules, Faculté des Sciences de Luminy, IN^{2}P^3-CNRS, F-13288 Marseille, France

M. Aleppo, M. Antonelli, F. Ragusa

Dipartimento di Fisica, Università di Milano e INFN Sezione di Milano, I-20133 Milano, Italy.

R. Berlich, V. Büscher, H. Dietl, G. Ganis, K. Hüttmann, G. Lütjens, C. Mannert, W. Männer, H.-G. Moser, S. Schael, R. Settles, H. Seywerd, H. Stenzel, W. Wiedenmann, G. Wolf

Max-Planck-Institut für Physik, Werner-Heisenberg-Institut, D-80805 München, Germany[16]

P. Azzurri, J. Boucrot, O. Callot, S. Chen, M. Davier, L. Duflot, J.-F. Grivaz, Ph. Heusse, A. Jacholkowska, M. Kado, J. Lefrançois, L. Serin, J.-J. Veillet, I. Videau,[12] J.-B. de Vivie de Régie, D. Zerwas

Laboratoire de l'Accélérateur Linéaire, Université de Paris-Sud, IN^{2}P^3-CNRS, F-91898 Orsay Cedex, France

G. Bagliesi,[12] S. Bettarini, T. Boccali, C. Bozzi, G. Calderini, R. Dell'Orso, I. Ferrante, A. Giassi, A. Gregorio, F. Ligabue, A. Lusiani, P.S. Marrocchesi, A. Messineo, F. Palla, G. Rizzo, G. Sanguinetti, A. Sciabà, G. Sguazzoni, R. Tenchini, C. Vannini, A. Venturi, P.G. Verdini

Dipartimento di Fisica dell'Università, INFN Sezione di Pisa, e Scuola Normale Superiore, I-56010 Pisa, Italy

G.A. Blair, J.T. Chambers, J. Coles, G. Cowan, M.G. Green, T. Medcalf, J.A. Strong, J.H. von Wimmersperg-Toeller

Department of Physics, Royal Holloway & Bedford New College, University of London, Surrey TW20 OEX, United Kingdom[10]

D.R. Botterill, R.W. Clifft, T.R. Edgecock, P.R. Norton, J.C. Thompson, A.E. Wright

Particle Physics Dept., Rutherford Appleton Laboratory, Chilton, Didcot, Oxon OX11 OQX, United Kingdom[10]

B. Bloch-Devaux, P. Colas, B. Fabbro, G. Faïf, E. Lançon,[12] M.-C. Lemaire, E. Locci, P. Perez, H. Przysiezniak, J. Rander, J.-F. Renardy, A. Rosowsky, A. Trabelsi,[23] B. Tuchming, B. Vallage

CEA, DAPNIA/Service de Physique des Particules, CE-Saclay, F-91191 Gif-sur-Yvette Cedex, France[17]

S.N. Black, J.H. Dann, H.Y. Kim, N. Konstantinidis, A.M. Litke, M.A. McNeil, G. Taylor

Institute for Particle Physics, University of California at Santa Cruz, Santa Cruz, CA 95064, USA[19]

C.N. Booth, S. Cartwright, F. Combley, M.S. Kelly, M. Lehto, L.F. Thompson
Department of Physics, University of Sheffield, Sheffield S3 7RH, United Kingdom[10]

K. Affholderbach, A. Böhrer, S. Brandt, J. Foss, C. Grupen, G. Prange, L. Smolik, F. Stephan
Fachbereich Physik, Universität Siegen, D-57068 Siegen, Germany[16]

G. Giannini, B. Gobbo
Dipartimento di Fisica, Università di Trieste e INFN Sezione di Trieste, I-34127 Trieste, Italy

J. Putz, J. Rothberg, S. Wasserbaech, R.W. Williams
Experimental Elementary Particle Physics, University of Washington, WA 98195 Seattle, U.S.A.

S.R. Armstrong, E. Charles, P. Elmer, D.P.S. Ferguson, Y. Gao, S. González, T.C. Greening, O.J. Hayes, H. Hu, S. Jin, P.A. McNamara III, J.M. Nachtman,[21] J. Nielsen, W. Orejudos, Y.B. Pan, Y. Saadi, I.J. Scott, J. Walsh, Sau Lan Wu, X. Wu, G. Zobernig
Department of Physics, University of Wisconsin, Madison, WI 53706, USA[11]

[1]Now at Harvard University, Cambridge, MA 02138, U.S.A.
[2]Supported by the Commission of the European Communities, contract ERBFMBICT982894.
[3]Also at Dipartimento di Fisica, INFN Sezione di Catania, Catania, Italy.
[4]Also Istituto di Fisica Generale, Università di Torino, Torino, Italy.
[5]Also Istituto di Cosmo-Geofisica del C.N.R., Torino, Italy.
[6]Now at LAL, Orsay, France.
[7]Supported by CICYT, Spain.
[8]Supported by the National Science Foundation of China.
[9]Supported by the Danish Natural Science Research Council.
[10]Supported by the UK Particle Physics and Astronomy Research Council.
[11]Supported by the US Department of Energy, grant DE-FG0295-ER40896.
[12]Also at CERN, 1211 Geneva 23, Switzerland.
[13]Supported by the US Department of Energy, contract DE-FG05-92ER40742.
[14]Supported by the US Department of Energy, contract DE-FC05-85ER250000.
[15]Permanent address: Universitat de Barcelona, 08208 Barcelona, Spain.
[16]Supported by the Bundesministerium für Bildung, Wissenschaft, Forschung und Technologie, Germany.
[17]Supported by the Direction des Sciences de la Matière, C.E.A.
[18]Supported by Fonds zur Förderung der wissenschaftlichen Forschung, Austria.
[19]Supported by the US Department of Energy, grant DE-FG03-92ER40689.
[20]Now at University of Geneva, 1211 Geneva 4, Switzerland.
[21]Now at University of California at Los Angeles (UCLA), Los Angeles, CA 90024, U.S.A.
[22]Now at SAP AG, D-69185 Walldorf, Germany
[23]Now at Département de Physique, Faculté des Sciences de Tunis, 1060 Le Belvédère, Tunisia.

1 Introduction

In e^+e^- collisions at LEP 2 energies, the trilinear WWγ and WWZ couplings can be probed with direct W-pair ($e^+e^- \to W^+W^-$), single W ($e^+e^- \to We\nu$) production or with photon production ($e^+e^- \to \nu\overline{\nu}\gamma(\gamma)$) [1,2]. In the WW channel a minimal set of five independent parameters is necessary to describe the Z and γ couplings to the W, assuming C and CP conservation. Usually a model-dependence is introduced to reduce this set to at most three parameters (e.g. the model with the parameters $\alpha_W, \alpha_{W\phi}, \alpha_{B\phi}$ [3]). Although the photonic channel is less sensitive to the couplings than the W pair and single W channels [4], it can resolve sign ambiguities and is therefore complementary. Constraints on the WWγ vertex have also been obtained at the Tevatron [5] within a slightly different theoretical framework.

The purpose of this letter is to set constraints on the WWγ trilinear couplings with a study of photonic events, using data collected by ALEPH at centre-of-mass energies ranging from 161 to 184 GeV and corresponding to a total integrated luminosity of about 80 pb^{-1}.

In the Standard Model, three processes contribute at tree level to the $\nu\overline{\nu}\gamma$ final state corresponding to the five diagrams shown in Figure 1.

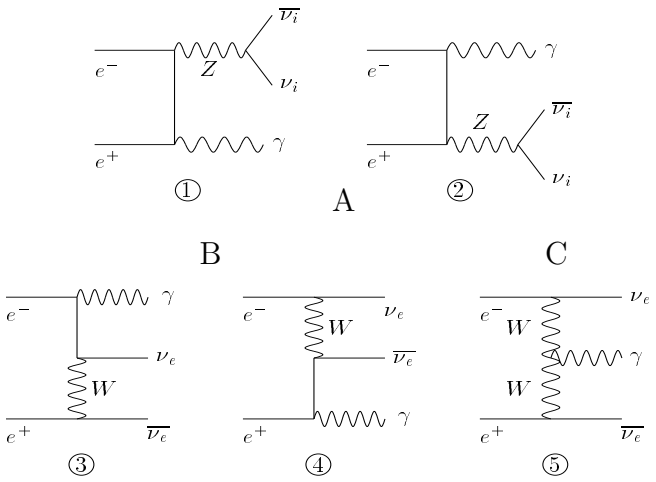

Figure 1: Feynman diagrams for $e^+e^- \to \bar{\nu}\nu\gamma$. Only the process C is sensitive to the WWγ couplings.

The WWγ vertex is present only in the last diagram, which contributes about 0.3% to the total Standard Model $e^+e^- \to \bar{\nu}\nu\gamma$ cross section, but which also leads to characteristic energy and angular distributions of the final state photons. A measurement of the total cross section, supplemented by a fit to these distributions, is therefore sensitive to the presence of an anomalous WWγ coupling.

This vertex can be described [3] by three C and P conserving parameters, g^1_γ, κ_γ and λ_γ, related to the following W boson properties:

$$\begin{aligned} \text{charge} \quad Q_w &= e g^1_\gamma \\ \text{magnetic dipole moment} \quad \mu_w &= \frac{e}{2m_w}(g^1_\gamma + \kappa_\gamma + \lambda_\gamma) \\ \text{electric quadrupole moment} \quad q_w &= \frac{e}{m_w^2}(\kappa_\gamma - \lambda_\gamma) \end{aligned}$$

In the Standard Model, these three parameters are equal to 1, 1 and 0, respectively, and their deviations from these values are parameterized as "anomalous couplings" Δg_γ^1, $\Delta\kappa_\gamma$ and λ_γ. Here, the electric charge of the W boson is assumed to be equal to that of the electron, thus fixing $g_\gamma^1 = 1$, while no further assumptions are made on κ_γ and λ_γ. The matrix element for the $e^+e^- \to \nu\overline{\nu}\gamma(\gamma)$ final state is a linear function of $\Delta\kappa_\gamma$ and λ_γ. Its implementation in the KORALZ Monte Carlo program [6], including initial state radiation of additional photons, is used throughout this analysis.

This letter is organized as follows. In Section 2, the aspects of the ALEPH detector relevant to this analysis are described. The event selection is presented in Section 3, and the fit of the data to the presence of anomalous WWγ couplings is discussed in Section 4. Section 5 gives the fitted values and the resulting constraints on $\Delta\kappa_\gamma$ and λ_γ; the systematic uncertainties are discussed in Section 6.

2 The ALEPH detector

The ALEPH detector and its performance are described in detail in [7, 8]. Here only a brief description of the properties relevant to the present analysis is given.

The central part is dedicated to the detection of charged particles. From the interaction point outwards, the trajectory of a charged particle is measured by a two-layer silicon strip vertex detector, a cylindrical drift chamber and a large time projection chamber (TPC). The three tracking detectors are immersed in a 1.5 T axial field provided by a superconducting solenoidal coil.

Photons are identified in the electromagnetic calorimeter (ECAL), situated between the TPC and the coil. It is a lead–proportional–wire sampling calorimeter segmented in $0.9^\circ \times 0.9^\circ$ towers read out in three sections in depth. It has a total thickness of 22 radiation lengths and yields an energy resolution of $\delta E/E = 0.18/\sqrt{E} + 0.009$ (E in GeV). Two independent readouts of the energy are implemented respectively on the cathode pads and on the anode wires of the ECAL. At low polar angles, the ECAL is supplemented by two calorimeters, LCAL and SiCAL, principally used to measure the integrated luminosity collected by the experiment, but used also here for vetoeing purposes.

The iron return yoke is equipped with 23 layers of streamer tubes and forms the hadron calorimeter (HCAL), seven interaction lengths thick; it provides a relative energy resolution of charged and neutral hadrons of $0.85/\sqrt{E}$. Muons are identified using hits in the HCAL and the muon chambers; the latter are composed of two layers of streamer tubes outside the HCAL.

The information from the tracking detectors and the calorimeters are combined in an energy flow algorithm [8]. For each event, the algorithm provides a set of charged and neutral reconstructed particles, called energy flow objects, used in the analysis.

3 Event samples and selection

The data were collected with the ALEPH detector at LEP at several centre-of-mass energies between 161 and 172 GeV in 1996, and between 181 and 184 GeV in 1997. The corresponding integrated luminosities are given in Table 1.

Table 1: Data samples.

Energy (GeV)	Luminosity (pb^{-1})	N events	
		Data	Expected
161	11.0	32	31.8
172	10.7	27	32.2
183	58.1	148	145.8
Total	79.8	207	209.8

3.1 Selections and cuts

Photon candidates are defined as described in [8]. Only events with no reconstructed charged particle tracks and at least one photon with an energy $E_\gamma > 0.1\sqrt{s}$ are considered; the trigger efficiency for such events is almost 100%. At most one hit is accepted in the muon chambers, to eliminate beam-related and cosmic ray muons. The loss of signal events with noisy muon chambers was estimated from events triggered at random beam crossings to be 3%. The timing of the energy deposition in the ECAL is checked to be consistent with the beam crossing time.

All events with at least 0.5 GeV detected below 14° from the beam axis are rejected, in order to remove radiative Bhabha events. The efficiency correction factor associated with this cut was estimated from events triggered at random beam crossings to be 3.5%.

The consistency between the energy measured from the ECAL pads and from the ECAL wires is checked. In case of leakage out of the ECAL, a localized energy deposit in the HCAL, E_{had}, associated to an ECAL cluster is added to E_γ, after correcting for the e/π ratio; only events with $E_{had}/E_\gamma < 10\%$ are kept. To reduce the remaining background, all but 2.5 GeV of the total energy is required to come from photon candidates.

At least one photon candidate is required to fulfil the conditions $\theta_\gamma > 20°$ and $p_{T\gamma}/E_{beam} > 0.1$. For multiphoton candidates, the additional photons are considered only if their energy exceeds $0.05\sqrt{s}$. The overall missing transverse momentum is required to be greater than 12 GeV/c. The last cut removes the remaining Bhabha events with radiation at large angle.

Table 1 shows the data samples used in this analysis. The numbers of selected events agree with the numbers expected from the SM cross sections determined with the KORALZ Monte Carlo. The cross section measured from the data at 183 GeV, with the present analysis and within the global kinematic cuts, is 3.45±0.30 pb, to be compared to the SM prediction of 3.40 ± 0.02 pb.

3.2 Monte Carlo simulation with KORALZ

The simulation uses a modified version of the KORALZ program, which includes the SM expectation (with electroweak corrections) as well as QED radiative corrections, and the contributions of anomalous coupling amplitudes with exact matrix element calculations [9]. The overall higher-order QED correction factor is around 1.4, but depends on the centre-of-mass energy. More than ten thousand simulated events are used for each energy.

To obtain a description of the anomalous couplings in the simulation, each event

is assigned a weight, which is a function of $\Delta\kappa_\gamma$ and λ_γ. This method provides the smallest uncertainty, as the statistical error corresponds only to the differences between the distributions produced from the Standard Model and those from anomalous matrix elements.

As the matrix element is linear in $\Delta\kappa_\gamma$ and λ_γ the cross section and the differential distributions are bilinear forms of $\Delta\kappa_\gamma$ and λ_γ. For each event it is thus sufficient to store weights for only six configurations in the $(\Delta\kappa_\gamma, \lambda_\gamma)$ plane, in order to compute any cross section or kinematic variable as a function of $\Delta\kappa_\gamma$ and λ_γ. The leading order amplitudes including these anomalous couplings are folded with higher order QED effects, following the procedure discussed in [10].

The Standard Model predicts that the cross section for the radiative return to the Z resonance decreases when the centre-of-mass energy increases, while the opposite is true for the W exchange. In case of anomalous contributions, the sensitivity of the cross section increases almost quadratically above 161 GeV.

The kinematic cuts have been chosen to optimize the sensitivity to the anomalous couplings $\Delta\kappa_\gamma$ and λ_γ. Figure 2 gives the statistical sensitivity, defined as the anomalous contribution divided by the statistical error on the SM expectation, as a function of the scaled energy variable $x_E = E_\gamma / E_{beam}$. The minimum of the sensitivity occurs around the

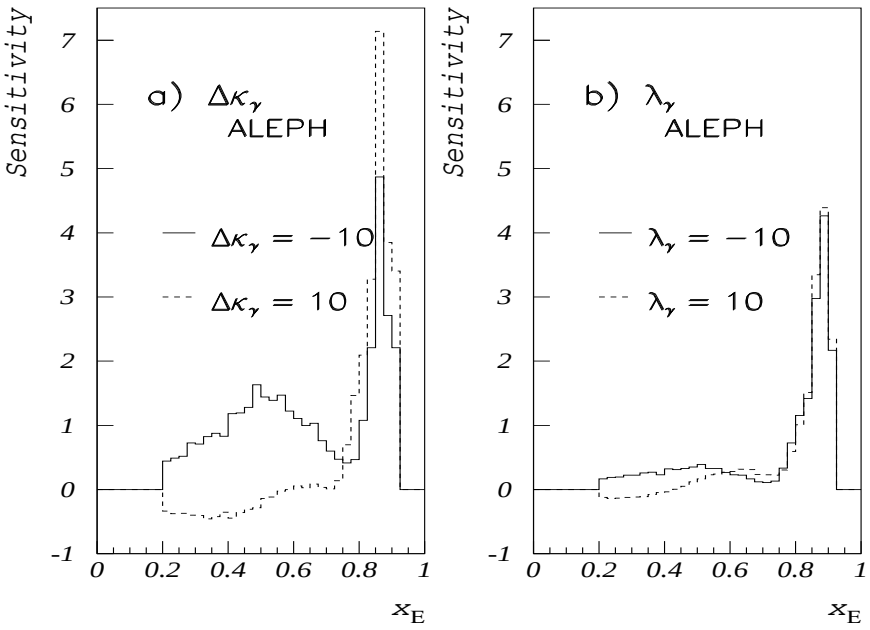

Figure 2: Statistical sensitivity of this analysis as a function of the scaled energy x_E at 183 GeV centre-of-mass energy: a) for $\Delta\kappa_\gamma$, b) for λ_γ. The sensitivity is defined as the anomalous contribution divided by the statistical error on the SM expectation. The solid and dashed histograms correspond to parameter values of -10 and $+10$, respectively. The single photon radiative return to the Z corresponds to $x_E = 0.75$.

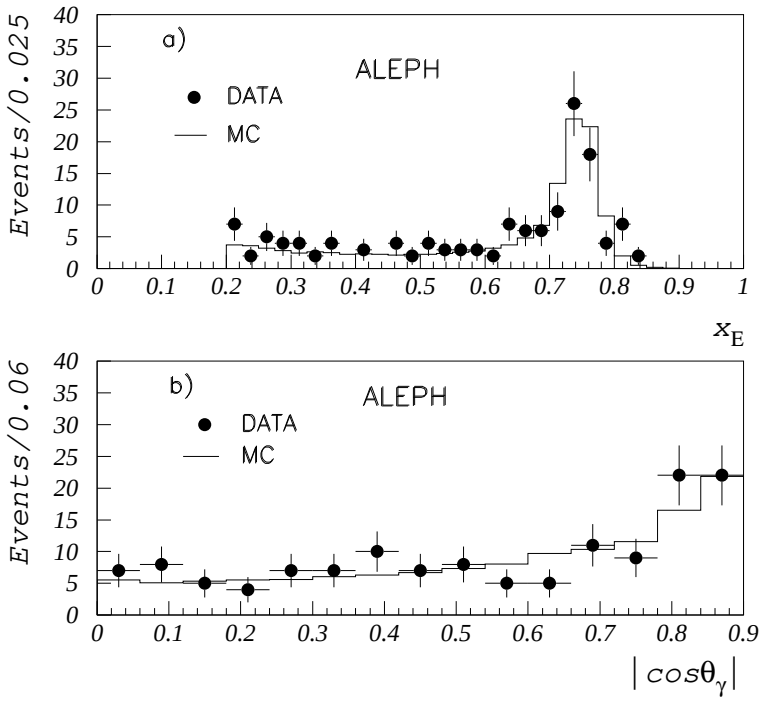

Figure 3: Inclusive distribution of a) the scaled energy x_E and b) the absolute value of the cosine of the polar angle of the photons, after all selections, for data and Monte Carlo at 183 GeV.

position of the Z return peak ($x_E = 0.75$). An important observation is that for $\Delta\kappa_\gamma > 0$ the differential cross section decreases almost linearly as a function of $\Delta\kappa_\gamma$ for events with $x_E < 0.75$, and increases quadratically above.

4 Likelihood fit

In addition to the observed number of events, two kinematic variables of the photon are used in the fit: the photon polar angle θ_γ and the scaled energy x_E. Figure 3 shows the distribution of x_E and $|\cos\theta_\gamma|$ for data, compared to the Standard Model predictions for $\sqrt{s} = 183$ GeV.

Two kinematic regions have been chosen for the fit, excluding the region of the Z peak return where the sensitivity to the anomalous couplings is minimal. Only photons with $|\cos\theta_\gamma| < 0.9$ are used for the fit to the shape of the distributions.

Defining $E_\gamma^{\mathrm{Z}} = (s - m_{\mathrm{Z}}^2)/2\sqrt{s}$, the two kinematic regions are the following:

- Region 1, low energy photons with $E_\gamma < E_\gamma^{\mathrm{Z}} - 3\Gamma_{\mathrm{Z}}$

  The contribution from higher order radiative corrections is described by an almost constant term obtained from the Monte Carlo simulation. The scaled variable x_E is

found to be as discriminant as the angular variable in the fit. Both are used for the $\Delta\kappa_\gamma$ fit, whereas λ_γ is determined only from the total cross section. The sensitivity to the λ_γ parameter in this kinematic region is very low.

- Region 2, high energy photons with $E_\gamma > E_\gamma^Z + 0.5$ GeV

  In this region, the higher order radiative corrections decrease the number of expected events by 30%. The scaled energy x_E is more discriminant than the angular variable, both variables being used in the fit of $\Delta\kappa_\gamma$ and λ_γ. It can be observed (Figure 2) that the sensitivity to λ_γ with x_E is similar to that of $\Delta\kappa_\gamma$.

Limits for anomalous coupling parameters have been derived from the generalized likelihood expression:

$$\log L = \log \frac{(N_{th}^{(1)})^{N_{obs}^{(1)}} e^{-N_{th}^{(1)}}}{N_{obs}^{(1)}!} + \log \frac{(N_{th}^{(2)})^{N_{obs}^{(2)}} e^{-N_{th}^{(2)}}}{N_{obs}^{(2)}!} + \sum \log P_i^{(1)} + \sum \log P_i^{(2)},$$

where $P_i^{(1)}$, $P_i^{(2)}$ are the probability density functions of observing event i with a given value of x_E and θ_γ in region 1 and 2 respectively, and $N_{th}^{(1)}$ and $N_{th}^{(2)}$ are the expected number of events in each region, including background. This likelihood formula contains two parts: the first one concerning the number of observed events, the second one being related to differential distributions for each kinematic region. The number of events used in the fit and those expected from the SM are given in Table 2.

The acceptance convoluted with the experimental resolution leads to correction factors to the cross sections of 1.10 for the first kinematic region and 0.7 for the second; these correction factors are constant (within $\pm 2\%$) in each region as $\Delta\kappa_\gamma$ or λ_γ vary.

The studies made with the KORALZ Monte Carlo show that the cross sections and distribution shapes vary differently in the two kinematic regions. For low energy photons the anomalous effects result from the interference term between the SM amplitude and the anomalous amplitude; the resulting variation is monotonic and linear for $\Delta\kappa_\gamma(\lambda_\gamma) > 0$ and $\Delta\kappa_\gamma(\lambda_\gamma) < 0$ and only one solution is expected for the $\Delta\kappa_\gamma$ and λ_γ fit. For the high energy photons, the variations are quadratic (due to a quadratic contribution of the anomalous amplitude) and one or two solutions are expected; the case of one solution corresponds to $\Delta\kappa_\gamma = 0$ or $\lambda_\gamma = 0$. This behaviour, important in the error determination, is discussed later when the error calibration procedure is presented.

Table 2: Number of events (N Events) entering the fit in the two kinematic regions. The number of expected events is estimated from the KORALZ cross sections, corrected for acceptance.

Kinematic region	N Events, Cross section fit		N Events, (x_E, θ) fit	
	Data	Expected	Data	Expected
Region 1	93	101.0	60	67.4
Region 2	30	32.8	23	25.6

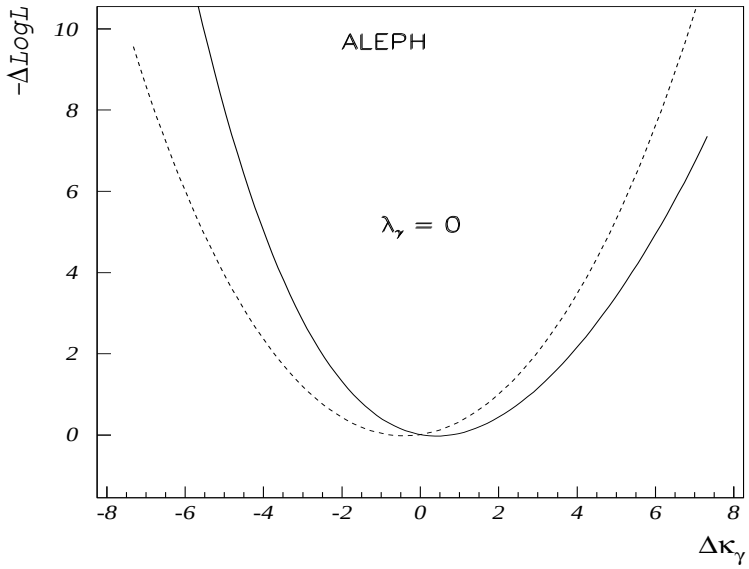

Figure 4: Likelihood curves for the fit of $\Delta\kappa_\gamma$ at $\lambda_\gamma = 0$ for the contribution of the cross section term (solid curve) and the shape term in x_E and θ (dashed curve).

5 Results

The likelihood functions are calculated globally for the cross section and on an event-by-event basis for the energy and angular distributions. Figure 4 displays the variations of the log-likelihood ($-\Delta$logL) corresponding to the fit of $\Delta\kappa_\gamma$ at $\lambda_\gamma = 0$, for the cross section and the distribution contributions. At present energies, the contributions of the cross section and of the shape variation terms are equally important for the fit of $\Delta\kappa_\gamma$. The result for λ_γ is dominated by the sensitivity to the shape in Region 2.

Figure 5 shows the ($-\Delta$logL) functions for $\Delta\kappa_\gamma$ fitted at $\lambda_\gamma = 0$, and for λ_γ fitted at $\Delta\kappa_\gamma = 0$ when the two contributions are merged. The results are:

$$\begin{aligned} \Delta\kappa_\gamma &= 0.05^{+1.15}_{-1.10}(\text{stat}) \quad \text{assuming} \quad \lambda_\gamma = 0 \\ \lambda_\gamma &= -0.05^{+1.55}_{-1.45}(\text{stat}) \quad \text{assuming} \quad \Delta\kappa_\gamma = 0 \end{aligned}$$

where the errors correspond to an increase of $-$logL by 0.5. The lower precision for λ_γ is expected since the exchanged W's are at a rather low momentum scale and the λ_γ term in the Lagrangian contains high powers of the W momentum.

The 95% C.L. limits derived from the one parameter fits are :

$$\begin{aligned} -2.1 < \Delta\kappa_\gamma < 2.2 \quad \text{assuming} \quad \lambda_\gamma = 0 \\ -3.0 < \lambda_\gamma < 3.1 \quad \text{assuming} \quad \Delta\kappa_\gamma = 0. \end{aligned}$$

The validity of these 95% C.L. limits have been checked using 100 Monte Carlo samples corresponding to the data luminosity, the analysis procedure described for the data being

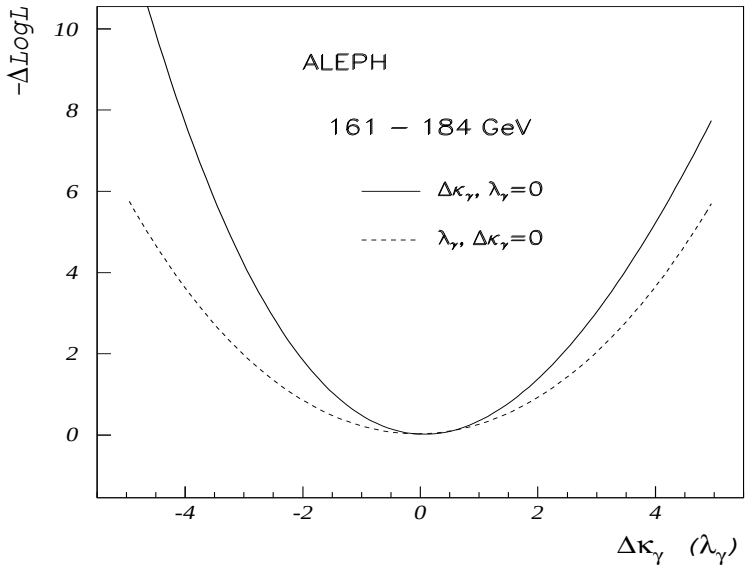

Figure 5: Likelihood curves for the fit of λ_γ at $\Delta\kappa_\gamma = 0$ (solid curve) and $\Delta\kappa_\gamma$ at $\lambda_\gamma = 0$ (dashed curve) for the sum of the cross section and distribution shape terms.

applied to each Monte Carlo sample. This study indicates that these errors are consistent with the frequentist interpretation, within 10% of their values, and do not benefit from favourable statistical fluctuations.

Figure 6 shows the 68% and 95% confidence level contours in the $(\Delta\kappa_\gamma, \lambda_\gamma)$ plane from a two-parameter fit. Although the two parameters are not independent, the confidence level contours are symmetric. This comes from the fact that the results are very close to 0, so that only one minimum is found. If the results were far away from the SM prediction, there could be several local minima, around which the two parameters would be correlated.

6 Systematic uncertainties

The contributions to the systematic uncertainty on the determination of $\Delta\kappa_\gamma$ are summarized in Table 3. The total systematic uncertainty is much smaller than the statistical one.

- The acceptance corrections were tested with different cuts in x_E and θ. This led to an uncertainty on the fit results as shown in Table 3.
- The main contribution to the systematic error in the present study comes from the energy calibration of high energy photons, which has been checked to be 1% with a large sample of $e^+e^- \to \gamma\gamma$ events.

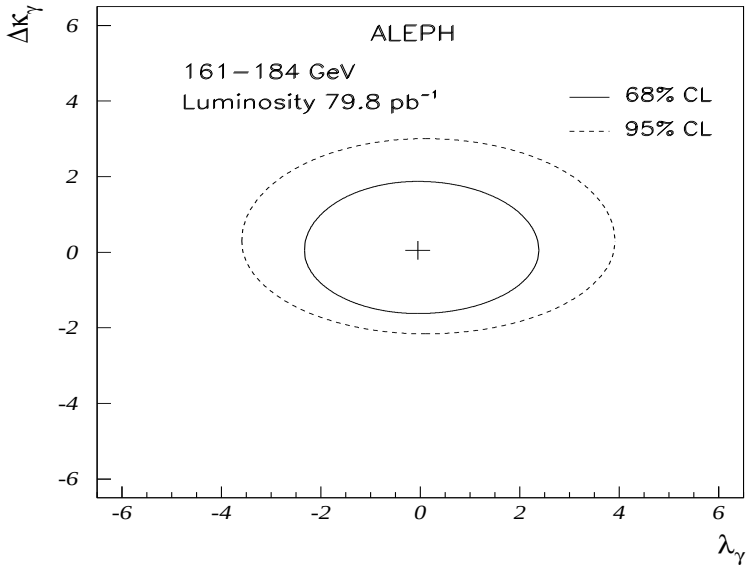

Figure 6: 68% and 95% confidence level contours in the $\Delta\kappa_\gamma, \lambda_\gamma$ plane.

- The possible contributions to the $e^+e^- \to \gamma(\gamma) + X$ channel, other than $X = \nu\overline{\nu}$, may come from radiative Bhabhas or $e^+e^- \to \gamma\gamma(\gamma)$ events. All such events in the Monte Carlo sample are eliminated by the angular and energy cuts.

- The KORALZ simulation of higher order effects gives a correction of about +100% for the SM cross section in Region 1, and about −30% in Region 2.

  A theoretical estimate of the error on these correction factors is about 5%. However, only comparisons with complete calculations from the exact matrix elements (not present in KORALZ) for the two and three hard bremsstrahlung photons would allow a satisfactory estimation of this uncertainty. A discussion of the uncertainty due to the implementation of the matrix elements with anomalous couplings for the multiphoton events is presented in [10].

Table 3: Contributions to the systematic uncertainty on fitted $\Delta\kappa_\gamma$, as explained in the text.

Origin of uncertainty	Region 1	Region 2
Acceptance corrections	±0.08	±0.08
Photon energy calibration ±1%	±0.10	±0.20
Background < 1 event	+ 0.05	+ 0.05
Model uncertainty < ±5%	±0.10	±0.15
Luminosity value ±0.6%	±0.03	±0.03
Total	±0.20	±0.30

The model uncertainty in introducing the anomalous couplings into the simulation has been checked. The reliability of the simulation of the Standard Model is discussed in [10].

- Another contribution to the uncertainty on the total cross section part of the fit is given by the luminosity error.

Other possible contributions to the systematic error, such as the statistical precision on the correction factors for muon rejection and energy deposition in the forward region of the detector, are negligible. For λ_γ, the basic errors are the same, one region only being used for the systematic error calculation.

7 Conclusions

The anomalous coupling parameters $\Delta\kappa_\gamma$ and λ_γ have been measured from single and multiphoton events in e^+e^- collisions between 161 and 184 GeV. The results from the fit to the cross sections and to the energy and angular distributions of the photons are

$$\begin{aligned} \Delta\kappa_\gamma &= 0.05^{+1.15}_{-1.10}(\text{stat}) \pm 0.25(\text{syst}) \\ \lambda_\gamma &= -0.05^{+1.55}_{-1.45}(\text{stat}) \pm 0.30(\text{syst}). \end{aligned}$$

The corresponding 95% C.L. limits including systematic errors are :

$$\begin{aligned} -2.2 < \Delta\kappa_\gamma < 2.3 \quad \text{assuming} \quad \lambda_\gamma = 0 \\ -3.1 < \lambda_\gamma < 3.2 \quad \text{assuming} \quad \Delta\kappa_\gamma = 0 \end{aligned}$$

These results are in good agreement with the Standard Model predictions and the uncertainty is largely dominated by the limited statistics of the data sample.

8 Acknowledgements

We thank and congratulate our colleagues in the CERN accelerator divisions for the successful operation of LEP2. We are indebted to the engineers and technicians in all our institutions for their contribution to the excellent performance of ALEPH. Those of us from non-member countries thank CERN for its hospitality and support. We would also like to thank J. Kalinowski for discussions and Z. Wąs for providing us with a Monte Carlo generator containing the gauge sector for the reaction $e^+e^- \to \nu\overline{\nu}\gamma(\gamma)$.

References

[1] G.V. Borisov, V.N. Larin and F.F. Tikhonin, *Zeit. Phys.* **C41** (1988) 287.

G. Couture, S. Godfrey, *Phys. Rev.* **D50** (1994) 5607.

[2] J. Abragam, J.Kalinowski and P.Sciepko, *Nucl. Phys.* **B339** (1994) 136.

F. Berends *et al.*, *Nucl. Phys.* **B301** (1988) 583.

[3] *Triple Gauge Couplings*, G. Gounaris *et al*, in *Physics at LEP2*, G. Altarelli, T. Sjöstrand and F. Zwirner, editors, CERN 96-01 (1996) 525.

[4] ALEPH Collaboration, *Measurement of Triple Gauge-Boson Couplings at 172 GeV*, *Phys. Lett.* **B422** (1998) 369.

DELPHI Collaboration, *Measurement of Trilinear Gauge Couplings in* e^+e^- *collisions at 161 GeV and 172 GeV*, *Phys. Lett.* **B423** (1998) 194.

L3 Collaboration, *Measurement of Mass, Width and Gauge Couplings of the W Boson at LEP*, *Phys. Lett.* **B413** (1998) 176.

OPAL Collaboration, *Measurement of triple gauge boson couplings from* W^+W^- *production at* $\sqrt{s} = 172$ *GeV*, *Eur. Phys. Journal* **C2** (1998) 607.

[5] The D0 Collaboration, S. Abachi *et al*, *Phys. Rev.* **D58** (1998) 3102.

[6] S. Jadach, B.F.L. Ward and Z. Wąs, *Comp. Phys. Comm.* **79** (1994) 503.

[7] ALEPH Collaboration, *ALEPH: A Detector for Electron-Positron Annihilations at LEP*, *Nucl. Instr. Meth.* **A 294** (1990) 121.

[8] ALEPH Collaboration, *Performance of the ALEPH Detector at LEP*, *Nucl. Instr. Meth.* **A 360** (1995) 481.

[9] D. Choudhbury and J. Kalinowski, *Unravelling the* $WW\gamma$ *and* WWZ *Vertices at the Linear Collider:* $\nu\overline{\nu}\gamma$ *and* $\nu\overline{\nu}q\overline{q}$ *final states*, MPI-PTH /96-73, IFT-96/17.

[10] A. Jacholkowska, J. Kalinowski and Z.Wąs, *Higher–order QED corrections to* $e^+e^- \to \nu\overline{\nu}\gamma$ *at LEP2*, CERN-TH/98-55, IFT/3/98, hep-ph/9803375, submitted to Eur. Phys. Journal C.